Silicon (2022) 14:5951–5959
https://doi.org/10.1007/s12633-021-01361-4

ORIGINAL PAPER

Gate All Around Dopingless Nanotube TFET Biosensor with $Si_{0.5}Ge_{0.5}$ – Based Source

Kosheen Wighmal [1] · Giridhar Peddi [1] · Apoorva [2] · Naveen Kumar [3] · S. Intekhab Amin [4] · Sunny Anand [1]

Received: 4 July 2021 / Accepted: 27 August 2021 / Published online: 13 September 2021

Abstract
Through this paper, we discuss how Tunnel Field Effect Transistors can be utilized for the detection of biomaterials hence acting as a biosensor. The device proposed is a 3-D Doping less Nanotube Tunnel Field Effect Transistor (DL-NT-TFET) device with a wrap-around gate or a Gate all around to provide maximum control over the charge carriers as surface control increases. The source (p+) and drain (n+) are shaped by utilizing Charge Plasma Technique in which Hafnium metal with work 3.9ev is utilized at the drain side and Platinum metal with work function 5.93 eV is utilized at the source side. This technique is used for simplification in the fabrication as there is no requirement for Doping. For introducing Biomaterial, a cavity is introduced under the gate at the source side. Different dielectric values ranging from k = 1, 2.9, 3.57 ,5,8,12,16,20 is analysed to study the variation in parameters like I_D -V_{GS} characteristics, subthreshold slope, electric field, carrier concentration etc. as a part of the results. The objective of our work is to propose a device with the least difficulty in fabrication and improved characteristics like high Ion, low subthreshold slope, high Ion/I off ratio etc.

Keywords Doping less · Nanotube TFET · Charge plasma · Biosensor

1 Introduction

Biosensors are devices which can detect proteins, bio molecules, DNA, glucose etc. and convert it into an electrical signal by exploiting the change in current with change in gate dielectric property of the TFET. Biosensors are an emerging tool in fields like clinical diagnosis [1], medical research, food control, environment monitoring [2] and detection of crime [3]. In FETs, the electrical field is a factor in controlling the conductivity of the channel. The gate dielectric plays a crucial role in sensitivity and Ion. FETs as Biosensor exploit this property by altering the gate dielectric because of deposition of different k biomaterials hence modifying the capacitance and therefore the Ion. FET based biosensors or Bio-FETs are simpler to fabricate, efficient and more sensitive as compared to other devices used for the same purpose. In the past numerous devices based on FETs, like Ion sensitive FET (ISFET) [4] in which charged molecules are present between the gate dielectric and ionic solution [5] and Dielectrically modulated FET (DMFET) in which the presence of charged particles immobilized in a cavity created between gate and channel cause change in electrical properties like capacitance, conductivity, Drain current, Ion/I off ratio etc. and hence were suitable to use as a biosensor [6]. But due to drawbacks like short channel effects, power supply when scaling down, MOSFETs as biosensors were explored. It was realized that the characteristics like drain current improved but still the issue of high leakage current and subthreshold slope not under 60mv/decade existed [7].

TFETs however appear to be more promising because of the Band-to-Band Tunnelling (BTBT) at the source channel interface and the charge flow from Drain to Source. In Band to Band Tunnelling the valence band of the p region and the conduction band of the intrinsic region get aligned together and the electrons flow from drain to source side through tunnelling [8]. On applying Gate voltage, V_{GS} this gap is decreased and flow of the current is increased hence On current increases. BTBT depends on the Tunnelling gap of the

✉ Sunny Anand
sunnyanand.42@gmail.com

[1] Department of Electronics and Communication Engineering, Amity University Noida, Noida, Uttar Pradesh, India

[2] IBM Pvt. Lmt, Bangalore, India

[3] University of Glasgow, Glasgow, Scotland

[4] Jamia Millia Islamia, New Delhi, India

material, Band gap of the source side metal and effective mass of the device. FETs are p-I-n structures having comparatively high On current to Off current (Ion /Ioff) ratio, low threshold voltage which is important for constant field scaling and are highly functional for low-power applications [9]. This paper proposes a Doping less Nanotube TFET (DLNT-TFET), a 3-D device, in which charge plasma technique is used to make drain and source regions without doping by using suitable work functions [10], platinum 5.93 eV at the source side and Hafnium 3.9 eV at the drain side. The charge plasma technique helps overcome the problem of uniform doping and makes the fabrication much simpler. Since one of the drawbacks of a Tunnel Field Effect Transistor (TFET) is low On current, to improve that various techniques can be applied, one of which is using a low energy gap material at the source side so that Tunnelling is easier as energy band gap gets reduced. In our device, we have incorporated this technique by taking $Si_{0.5}Ge_{0.5}$ [11] which has low band gap as compared to pure Si [12]. Nanotube is basically a thin, hollow cylindrical structure or tube which can carry a current up to 10^{9} A/cm^2 in the cross-section and has advantages like increased gate control, ease in fabrication, good scale down properties, higher drain current, low leakage current. For application as a biosensor, a cavity has been made under the gate metal as shown in Fig. 2. In this work we study neutral biomaterials with different k values ranging from 1, 2.9, 3.57, 5, 8, 12, 16, and 20. The adjustment in dielectric is directly proportional to change in capacitance which is directly proportional to change in current flow. The results are observed and plotted for two devices, one without the cavity and the other with cavity to understand the changes when biomaterials are introduced.

2 Device Structure and Parameters

The 2-D device structures with and without cavity have been shown in Fig. 1(a) and (b) respectively. The 3-D architecture of the device has been represented in the Fig. 2. The parameters have been exhibited in Table 1. The device is made in a vertical nanotube fashion and is doping less. The total length of the structure is 60nm and the width of the structure is 13 nm. The source channel and drain are made on 5nm Silicon body. Source side is made up of a low band-gap material $Si_{0.5}Ge_{0.5}$.[12] Use of charge plasma technique is done to create source and drain. Platinum with work function 5.93 eV is used at the source side and Hafnium with work function 3.9 eV is implemented at the drain side. The use of higher metal work function accumulates positive charge carriers (holes) at the source side and a lower work function metal accumulates electrons (i.e., negatively charged particles) at the drain side. As we know for charge plasma technique, the width of the silicon body should be less than the Debye's length [13], i.e., LD = $[(\varepsilon Si.Vt)/(qN)]^{1/2}$, where, V_T is the threshold voltage and εSi and N are the dielectric constant and the intrinsic carrier concentration of the bulk silicon. The device parameters like thickness and choice of metal electrodes allow us to use charge plasma technique. The device has an intrinsic channel region with Silicon body. The metal used at the gate is Aluminium with 4.2 eV as work function. Metal electrodes contribute in reducing ambipolar or leakage current. The gate is an all-around structure in a tube manner to enhance the control over the device [14]. The gate is been mounted upon a layer of SiO_2.The thickness of gate oxide is 1.5nm and SiO_2 is used as the gate oxide. The electrodes are surrounded by SiO_2 in the shell& the core. The top right area adjacent to source region has a dielectric constant of air (i.e. k = 1) [15]. The spacer length taken is 5nm both at the shell& the core side. The length of the channel is 20nm and the width of the channel is 5nm. The small source spacer length helps keep low gate –source capacitance coupling and is used as a technique to improve the results. The small spacer length reduces the thickness of the depletion layer& develops a high electric field at the source – channel interface hence improving Ion. The Mole fraction for SiGe is taken to be 0.5 for maximum performance. For bio sensing application, a cavity of length 10nm and width 3.5nm has been created the gate at the

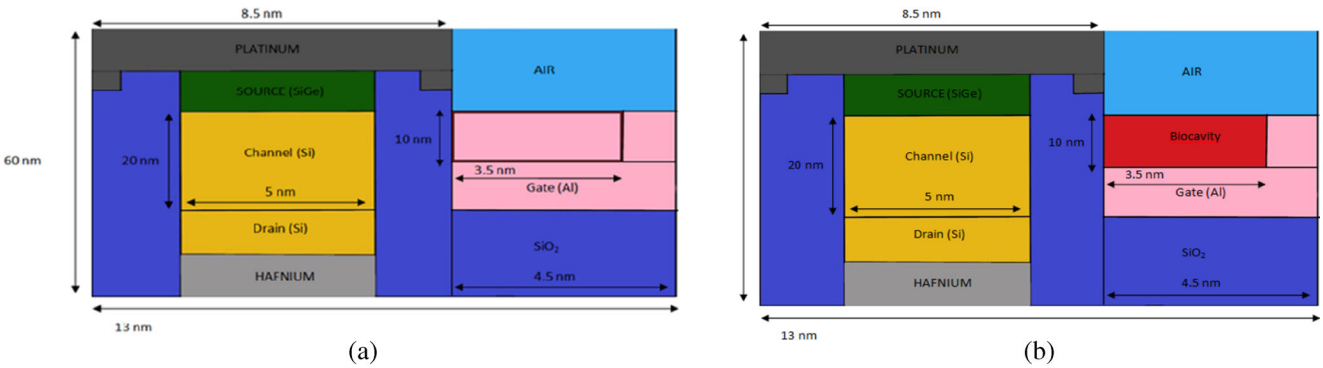

Fig. 1 2-D Device structure (**a**) Without cavity (**b**) With cavity

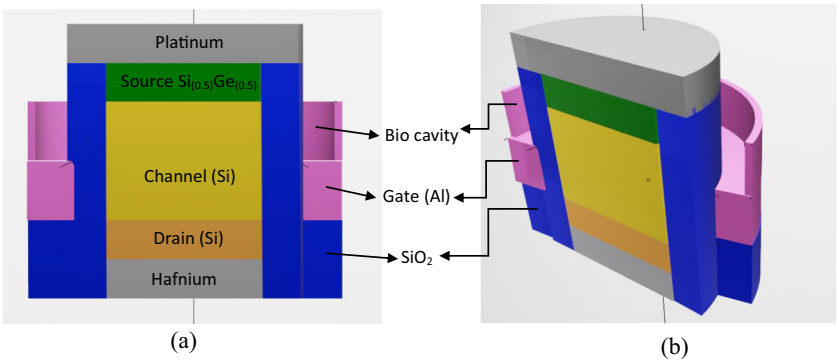

Fig. 2 (**a**) Crosssection view of 3D structure of the Biosensor. (**b**) Angled view of 3D structure

source channel interface. For $Si_{0.5}Ge_{0.5,\ the}$ tunnelling masses me. Tunnel = 0.19 mh.tunnel = 0.167 and for Si, me. Tunnel = 0.22 and mh. tunnel = 0.12.

3 Materials and Methods

We have used Lombardi mobility model at 300 K to calculate at constant voltage and temperature. Shockley–Read–Hall (SRH) generation-recombination model is used to include the leakage current and effect because of mobility in device. Non local band to band tunnelling model is used to incorporate the spatial movement of charge carriers. We the calculations based on Newton trap method. Since the channel width is 5nm we have used Quantum models. The technique implemented in our work to detect bio molecules is label detection technique. We have used SILVACO ATLAS for design & simulation of our device. We used ORIGINEPRO to plot our graphs for our graphed results [16].

4 Results and Discussion

The parameters like ON state current, capacitance, carrier concentration, electric field have been discussed in this section. The results have been calculated for both devices, including and noy including the cavity and compared at end.

Table. 1 Parameters used for simulation of proposed device

Parameters of the device	Values in nm
Total Length	60 nm
Total Width	13 nm
Length of channel	20 nm
Width of channel	5 nm
Length of cavity	10 nm
Width of cavity	3.5 nm
Length of Gate Oxide	20 nm
Width of Gate Oxide	1.5 nm

4.1 Results of Proposed Device

In this proposed article we are going to examine the results of our Silicon Germanium source-based Nanotube Tunnel FET Biosensor. In our device first let's examine the tunnelling property of our proposed device. Tunnelling property is examined by Wentzel-Kramer-Brillouin (WKB) approximation [17].

$$T_{\mathrm{WKB}} \approx \exp\left(-\frac{4\lambda\sqrt{2\mathrm{m}^*}\sqrt{\mathrm{E}_\mathrm{g}^3}}{3\mathrm{qh}\left(\mathrm{E}_\mathrm{g}+\Delta\Phi\right)}\right) \tag{1}$$

From this formula Eg is considered as energy band gap. Where E.g., decreases tunnelling probability increases. λ is the screening length of the device, and effective mass is described as m*. the potential difference of channel conduction band and source valence band is represented as ΔΦ. From Eq. (1) we can note that as effective mass and screening length decreases the tunnelling probability increases [18].

$$\lambda = \sqrt{\frac{\epsilon_{\mathrm{Si}}}{\epsilon_{\mathrm{ox}}} t_{\mathrm{Si}} t_{\mathrm{ox}}} \tag{2}$$

Since we are using tunnel FET the tunnelling probability should be accurate and efficient enough. So, λ can be suppressed by using high dielectric material 'k' as gate oxide in the devise which leads to greater capacitance around the channel. The electrostatic conditions of our device, in terms of Energy band, electric field and the transfer characteristics is shown in the form of graphs and discussed in this section.

The graph of the Energy band (in both ON and OFF state) is shown in Fig. 3(a) when our proposed device is taken under

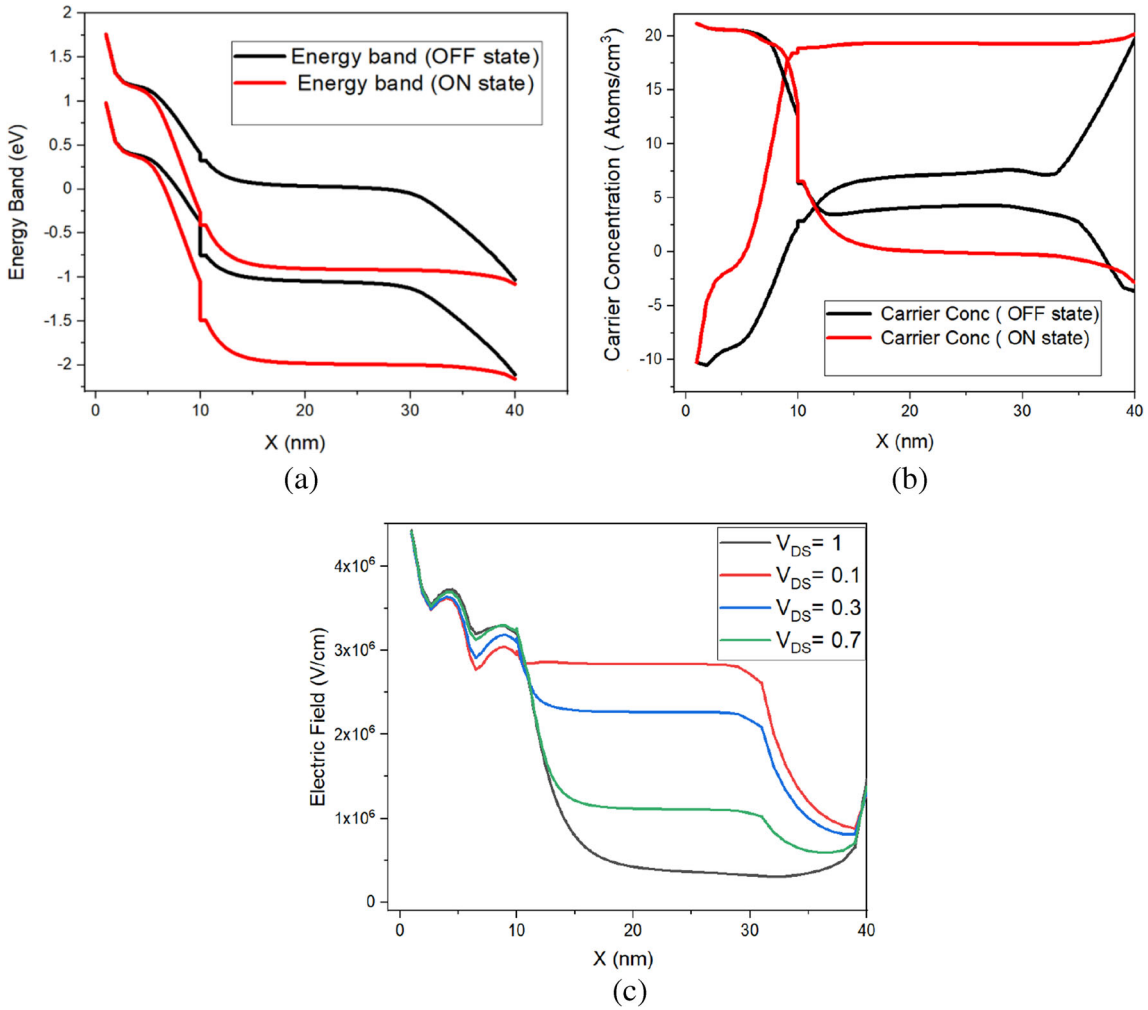

Fig. 3 (**a**) Energy Band Diagram (**b**) Carrier concentration (**c**) Electric Fields along the length of our device at OFF state ($\mathbf{V_{GS}}$ = 0 V, $\mathbf{V_{DS}}$ = 1 V) and at ON state ($\mathbf{V_{GS}}$ = 1.0 V, $\mathbf{V_{DS}}$ = 1 V)

consideration in the OFF state ($\mathbf{V_{GS}}$ = 0 V, $\mathbf{V_{DS}}$ = 1 V), we can note that the space between the valence band and conduction band at the position where the source and the channel of our device are meeting i.e., at 10 nm, so it is difficult for the electrons (e^-) to the tunnel. But when we consider our device at ON state($\mathbf{V_{GS}}$ = 1.0 V, $\mathbf{V_{DS}}$ = 1 V), the gap at 10nm is less compared to off state's gap and the tunnelling of the electron is done, we can conclude this by looking at the carrier concentration of our proposed device which is represented in Fig. 3(b) In the OFF state the electron concentration at drain(30nm -40nm) is from 10^{-10} cm^3 – 10^{20} cm^3 and electron concentration at the source is 10^5 to 10^{20} cm^3 this is because of charge plasma induction at the source side, so there might be some minority charge carriers when we compare it to the ON state, the concentration levels of the device increases as we can observe it in Fig. 3(b) the concentration of electrons (e^-) remains constant i.e. at 10^{20} cm^3 at the channel and drain, Since we observed the change in the concentrations of electrons and holes we can also observe the changes in Electric fields at different gate voltages i.e. in Fig. 3(c). At $\mathbf{V_{GS}}$ = 0.1 V, 0.3 V, 0.7 V, 1 V and we can note that the electric field at channel is higher at $\mathbf{V_{DS}}$ =0.1vand decreases gradually as $\mathbf{V_{DS}}$ increases [19].

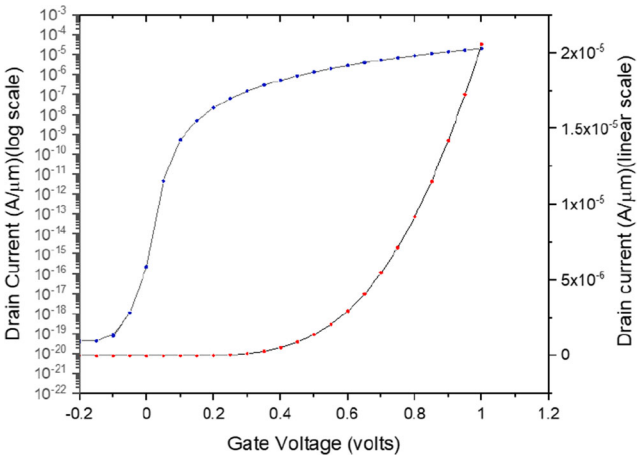

Fig. 4 Transfer Characteristics of Silicon Germanium core-shell Doping less Nanotube Tunnel FET

Now let's observe how the transfer Characteristics of our device is obtained as shown in Fig. 4. It displays the comparison between Gate voltage and drain current these results are calculated at $\mathbf{V_{GS}}$ = 1 V and $\mathbf{V_{DS}}$ at = 1 V. On the linear scale we obtain the drain current of 10^{-5} A/ μm. These results are collated with the reference work [20]. It is noted that our device which we proposed has less complexity in fabrication without any compromise in I_D (Drain current) in fact we can attain higher drain current as we introduced charge plasma technique and changed the effective mass of the electrons and holes by changing the source to SiGe.

Now let's look at the results of various parameters of the device like switching rate of our device (sub-threshold slope) by changing the work function of gate, source and ON state current and Ion/I off ratio of our proposed device as shown in Fig. 5(a), (b) and (c). When we vary the work function of the gate from 4.2 eV to 4.9 eV we can see that Average sub threshold increasing as we increase the work function but when we observe the ON state current, it is decreasing as the gate work function is increasing. We can observe that sweet spot of our device is at approx. 4.5 eV of the gate work function, so it is obvious that the gate work function of our proposed device is approx. 4.5 eV as you can see in Fig. 5(a). Now considering sensitivity of the device with channel length and A_{vg} SS (Average Sub threshold-Slope), as the length of the channel increases the sensitivity of the devise is increasing and the A_{vg} SS is decreasing so we chose the channel length of our device to be at 20nm for reducing the complexity of the fabrication, as shown in Fig. 5(b). Now looking at work function of the source and comparing it to A_{vg} SS and ON-state current we can see that at the source work function 5.9 eV is the sweet spot where A_{vg} SS and on state current are in balance so we chose the work function of our source metal to be 5.9 eV. Average Sub threshold of the device is calculated by using (1) [21].

$$\text{AverageSS} = \frac{V_t - V_{OFF}}{\text{Log}V_t - \text{Log}V_{OFF}} \tag{3}$$

In the equation the threshold voltage is calculated by using constant current method. And we can note that the A_{vg} sub threshold slope is less 60mV/decade [22].

4.2 Results of Proposed Device With Bio-cavity

In this part of the paper let's discuss the Energy band gap, Transfer Characteristics Electric field of our proposed device with varying k values of the Biomolecules and filling the cavity at different levels i.e. 10 %, 25 %, 50 %, 75 %,90 %. In Fig. 6(a) we can notice that Energy bands vary as the dielectric changes in ON state and we can see that the band changes as the dielectric increases& the band gap remains almost same for the change in the dielectric. The chemicals used with dielectric K = 3.57 is 3-aminopropyltriethoxysilane, K = 1 is air, K = 8 is for proteins and the biomolecules filled the cavity at 100 %. Now considering the Transfer Characteristics of our proposed Biosensor ant taking two different K values (1,3.57) the drain current increases as dielectric constant increases, since as k increases the capacitance increases as shown in the formula (3) and as capacitance increases the drain current increases.

$$C = Q/V$$

Now considering the Electric field across our device we can see that as dielectric increases, the Electric field intencity increases as shown in Fig. 6(c) As a result the drain current increases. Which helps us differentiate different biomolecules, which the planed intention of the Biosensor. Now let's discuss the different Transfer Characteristics of the Biosensor at 50 % filled cavity as shown in Fig. 7 and from this graph we can observe that as dielectric (k) increases the drain current increases constantly as k changes, for example let's consider at K = 1 and 2.9 at Gate voltage 1 V increases constantly as the value of I_D (Drain current) increases from K = 16 and 20 at V_g(Gate Voltage)1 V.Now considering the I_D -V_{GS} curve characteristics our proposed biosensor at the uniform dielectric k = 12 but filing the cavity at different levels i.e. at 10 %, 25 %, 50 %, 75 %, 90 % and from the observation we can see that as the cavity is filled with biomolecules is increased the drain current increases which is based on the same principle as Eq. 3 i.e. as capacitance increases the drain current increases automatically. In this device the channel length remains unchanged and there is no change in gate work function and source work function.

As we observe from Fig. 8, at V_{GS} = 1v and dielectric(k) = 12, with increase in percentage of the cavity filled from 10 to 90 %, the drain current increases. We observe the maximum drain current is when the cavity is 90 % filled i.e., $I_D \approx 6 \times 10^{-7} Amp$ and the min I_D (Drain current) is when the cavity is 10 % filled i.e. $I_D \approx 0.8 \times 10^{-7} Am$ p.

The sensitivity of a device is considered to be a crucial factor while measuring the performance of any device. So, for this biosensor we used drain current sensitivity to measure the performance of the biosensor.

$$\text{Sensitivity} = \frac{I_D(\text{bio}) - I_D(\text{air})}{I_D(\text{air})}$$

The sensitivity of the device is given by the ratio between I_D(drain current) of our device when the cavity filled with air to the difference between the drain currents when the cavity filled with bio molecules and cavity filled air respectively.

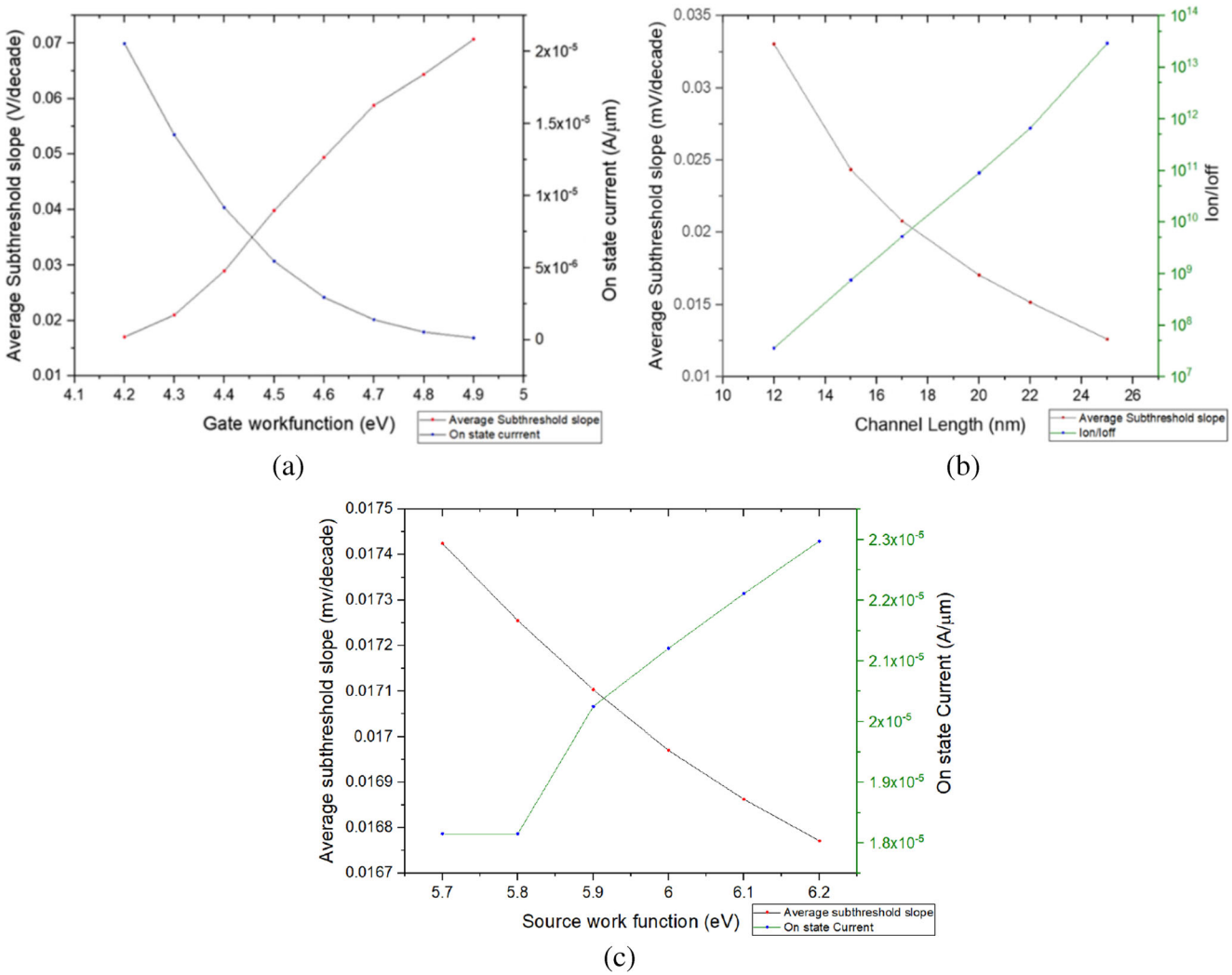

Fig. 5 (**a**) Gate Work function from 4.2 eV to 4.9 eV with respect to average SS and On state current, (**b**) channel length with respect to average SS and Ion/I off, (**c**) work function of the source w.r.t average SS and On state current

Where I_D (bio) = drain current with biomolecules and I_D (air) = drain current without biomolecules.

To explain about Fig. 9 it is generally the plot between the channel length (X nm) and the Electric filed (V/cm) along with these we have also included the behaviour of the Electric filed with IF charges present across the channel length, so as we observe as the plots of Fig. 9 as the channel length increases the electric field decreases based on the positions on source, channel, drain since the source will be the region where electrons are generated and manage, hence the electric field is higher at initial stages of channel length, considering the source being towards the left of the channel (i.e. before 0nm of X). When IF charge is included at the channel the electric filed stays almost inversely proportional that is all channel length increases electric field decreases. We also plotted the behaviour of electric field by using different IF charge values.

Figure 10 shows the drain current sensitivity characteristics of the biosensor of channel length 40 nm at dielectric at the cavity being 3.57 and 2.1 and air is taken into consideration. The sensitivity increases as the drain current linked with dielectric value; it is seen that the sensitivity increases as the drain current increases. The drain current sensitivity of the bio sensor is direct relationship to the ability of the our sensor to sense the biomolecules

5 Conclusion

In this article, we proposed Silicon Germanium source -based core-shell Gate All Around Doping less Nanotube Tunnel Field Effect Transistor and it is been analysed, examined, referred. The analysed readings reveal the procedure and reducing the complication of the device manufacturing and

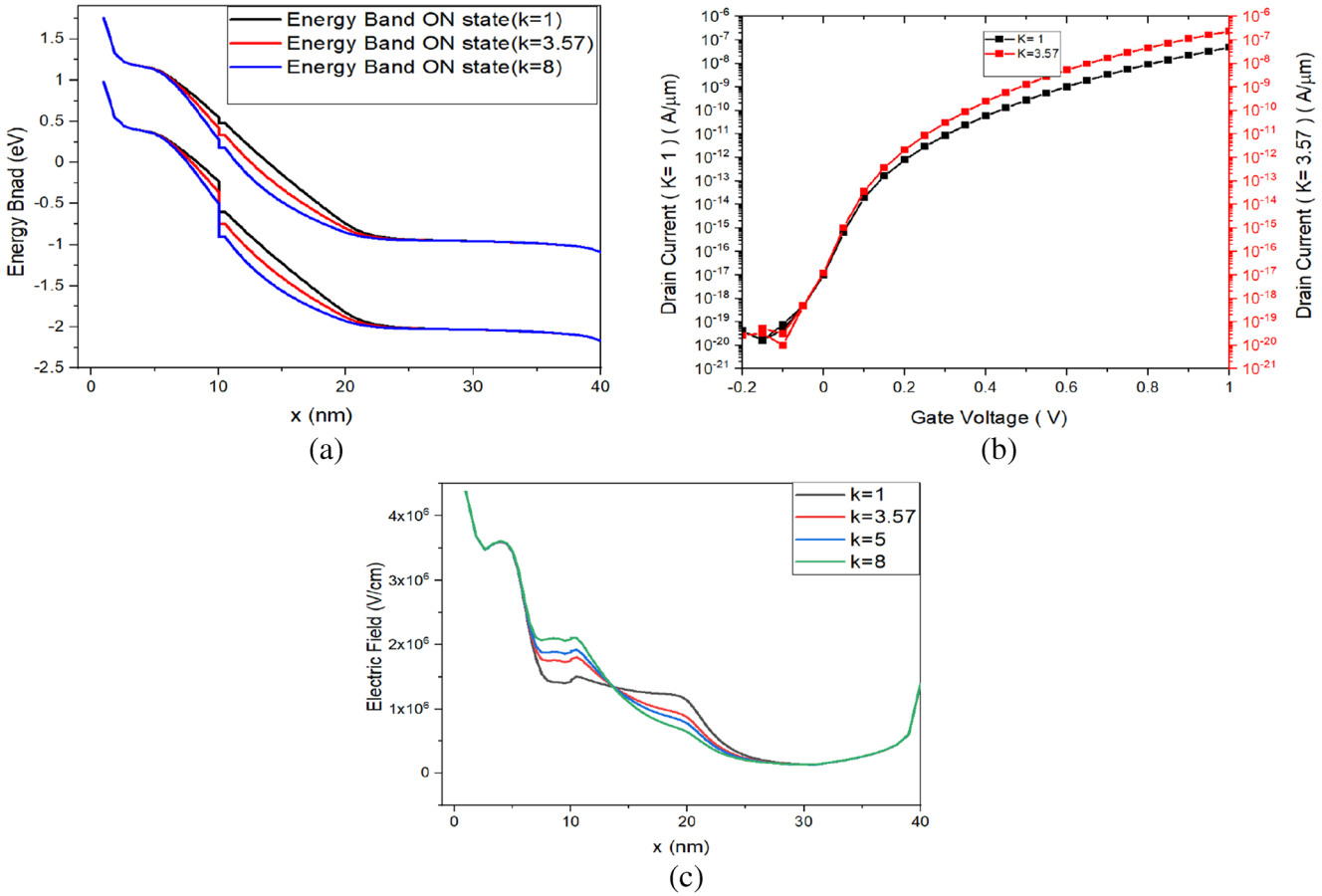

Fig. 6 (**a**) Energy band diagrams of the biosensor proposed at various K values (1,3.75,8), (**b**) Transfer characteristics of biosensor proposed at different k values (1, 3.57), (**c**) Electric fields of the biosensor proposed at different k values (1,3.57,5,8)

obtain the optimal drain current 10^{-5} A/ μm and used suitable channel length and feasible work functions of the gate, drain metal and source metal which makes the fabrication easier without compromising the cons of the biosensor. We tested this device on neutral biomolecules only.

The proposed device can work at any level of the cavity filled with biomolecules. With this we can conclude that the device suitable for its need as a Biosensor.

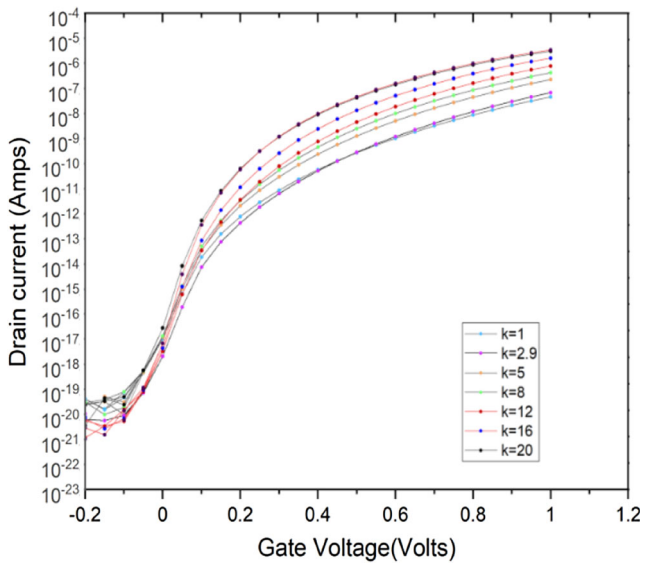

Fig. 7 Transfer Characteristics of the proposed Biosensor at different dielectrics (k) at 50 % cavity filled

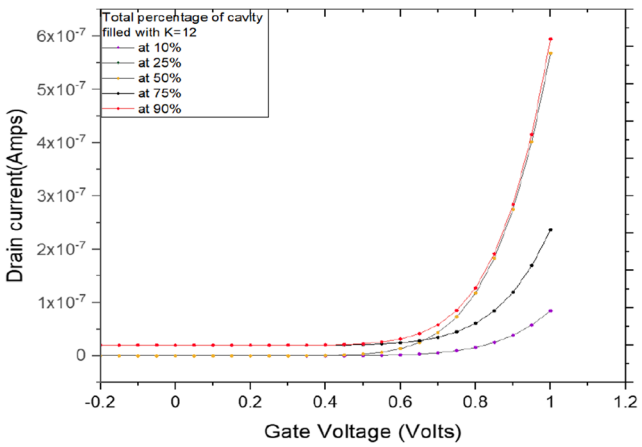

Fig. 8 Transfer characteristics of the proposed Biosensor at cavity filled at various percentages and the dielectric remaining constant at k = 12

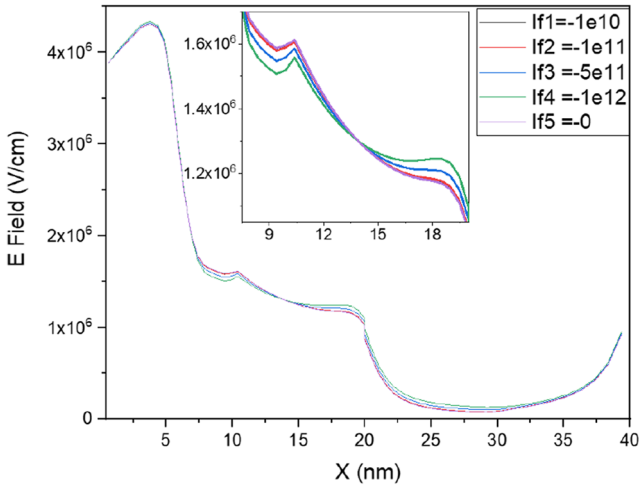

Fig. 9 Plot of Electric field Vs channel length (nm) with varied IF charge

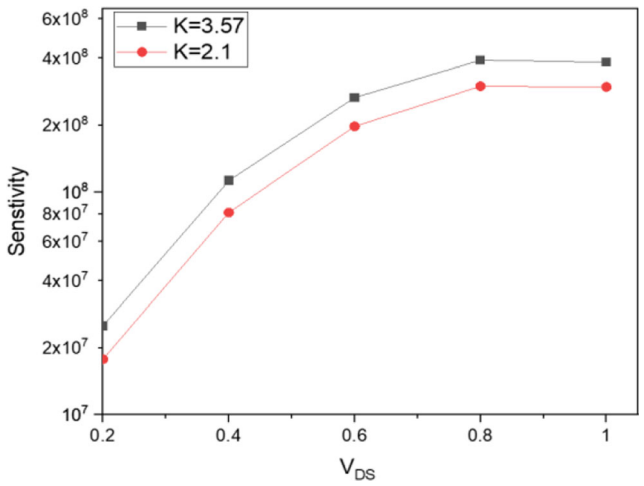

Fig. 10 Sensitivity plot of cavity length which is 40 nm

Author Contributions Kosheen Wighmal: Simulation, TCAD Software, Writing- Original draft preparation.

Peddi Giridhar: TCAD Software, Writing- Original draft preparation.

Apoorva: Simulation, Data curation and Revision.

Naveen Kumar: Simulation, TCAD Software, Logical-Methodology, conceptualization.

S. I. Amin: Revision and Supervision, Validation.

Sunny Anand Simulation, TCAD Software, Writing and Editing, computations.

Data Availability Not applicable.

Declarations

Ethics Approval and Consent to Participate Not Applicable.

Consent for Publication Not Applicable.

Competing Interests Not Applicable.

Disclosure of Potential Conflicts of Interest No conflicts to report.

Research involving Human Participants and/or Animals Not applicable.

Informed Consent Not applicable.

References

1. Wang J (1999) Amperometric biosensors for clinical and therapeutic drug monitoring: a review. J Pharm Biomed Anal 19:47–53
2. Rodriguez-Mozaz S, Lopez de Alda MJ, Barceló D (2006) Biosensors as useful tools for environmental analysis and monitoring. Anal Bioanal Chem 386:1025–1041
3. Shin J, Choi S, Yang J-S, Jung AI, Chemical B (2017) Smart forensic phone: colorimetric analysis of a bloodstain for age estimation using a smartphone. Sensors Actuators 243:221–225. https://doi.org/10.1016/j.snb.2016.11.142
4. Bergveld P (1970) Development of an ion-sensitive solid-state device for neurophysiological measurements. IEEE Trans Biomed Eng BME 17(1):70–71. https://doi.org/10.1109/TBME.1970.4502688
5. Stern E et al (2007) Label-free immune detection with CMOScompatible semiconducting nanowires. Nature 445:519–522
6. Im H, Huang XJ, Gu B, Choi YK (2007) A dielectric-modulated field-effect transistor for biosensing. Nat Nanotechnol 2:430–434. https://doi.org/10.1038/nnano.2007.180
7. Koswatta SO, Lundstrom MS, Nikonov DE (2009) Performance comparison between pin tunnelling transistors and conventional MOSFETs. IEEE Trans Electron Devices 56:456–465. https://doi.org/10.1109/TED.2008.2011934
8. Bhuwalka K, Schulze J, Eisele I (2005) Scaling the vertical tunnel FET with tunnel bandgap modulation and gate work function engineering. IEEE Trans Electron Devices 52(5):909–917. https://doi.org/10.1109/TED.2005.846318
9. Choi WY, Park BG, Lee JD, Liu TK (2007) Tunneling field effect transistors with subthreshold swing less than 60mV/dec. IEEE Electron Device Lett 28(8):743–745. https://doi.org/10.1109/LED.2007.901273
10. Kumar MJ, Janardhanan S (2013) Doping-less tunnel field effect transistor: Design and investigation. IEEE Trans Electron Devices 60(10):3285–3290. https://doi.org/10.1109/TED.2013.2276888
11. Gurmeet Singh S, Intekhab Amin S, Anand RK, Sarin (2016) Design of Si0.5Ge0.5 based tunnel field effect transistor and its performance evaluation. Superlattice Microst 92:143–156, ISSN 0749–6036. https://doi.org/10.1016/j.spmi.2016.02.027, https://www.sciencedirect.com/science/article/pii/S0749603616300702
12. Wang P-Y, Tsui B-Y (2013) Six Ge1 – x epitaxial tunnel layer structure for p2-channel tunnel FET improvement. IEEE Trans Electron Devices 60(12):4098–4104. https://doi.org/10.1109/TED.2013.2287633
13. Anand S, Sarin RK (2016) Analog and RF performance of dopingless tunnel FETs with Si0.55Ge0.45 source. J Comput Electron 15:850–856. https://doi.org/10.1007/s10825-016-0859-5
14. Boucart K, Ionescu AM (2007) Double-gate tunnel FET with highκ gate dielectric. IEEE Trans Electron Devices 54(7). https://doi.org/10.1109/TED.2007.899389
15. Fahad HM, Smith CE, Rojas JP, Hussain MM. Silicon nanotube field effect transistor with core–shell gate stacks for enhanced high-performance operation and area scaling benefits. Nano Lett 11(10):4393–9. https://doi.org/10.1021/nl202563s
16. Anand S, Singh A, Amin SI, Thool AS (2019) Design and performance analysis of dielectrically modulated doping-less tunnel FET-

based label free biosensor. 19(12):4369–4374. https://doi.org/10.1109/JSEN.2019.2900092
17. Anam A, Anand S, Amin SI (2020) Design and performance analysis of tunnel field effect transistor with buried strained $Si_{1-x}Ge_x$ source structure based biosensor for sensitivity enhancement. IEEE Sens J 20(22):13178–13185. https://doi.org/10.1109/JSEN.2020.3004050
18. Silvaco International (2010) ATLAS User Manual 2010. Silvaco International, Santa Clara
19. Anand S, Sarin RK (2016) An analysis on ambipolar reduction techniques for charge plasma based tunnel field effect transistors. J Nanoelectron Optoelectron 11(4):543–550. https://doi.org/10.1166/jno.2016.1922
20. N.Kumar U, Mushtaq SI, Amin (2019) Design and performance analysis of dual-Gate allaround Core-Shell Nanotube TFET. Superlattice Microstruct 125:356–364. https://doi.org/10.1016/j.spim.2018.09.012
21. Anand S, Amin SI, Sarin RK (2016) Analog performance investigation of duel electrode based doping-less tunnel FET 15(1):94–103. https://doi.org/10.1007/s10825-015-0771-4
22. Shreya S, Khan AH, Kr N, Amin I, Anand S. Core-shell junctionless nanotube tunnel field effect transistor: design and sensitivity analysis for biosensing application. https://doi.org/10.1109/JSEN.2019.2944885